Dissociation Kinetics of Actinomycin D from Oligonucleotides with Hairpin Motifs†

Fu-Ming Chen,* Christy M. Jones,‡ and Quentisha L. Johnson‡

Department of Chemistry, Tennessee State University, Nashville, Tennessee 37209-1561

Received December 29, 1992; Revised Manuscript Received March 23, 1993

ABSTRACT: The dissociation of 7-aminoactinomycin D (7-AM-ACTD) from d(ATGCATATGCAT), d(ATGCAT-T-ATGCAT), or d(ATGCAT-A-ATGCAT) at 20 °C cannot be adequately described by a single-exponential decay and requires a fit with two rate constants. The relative contributions of these two rate processes and their temperature dependence can be attributed to the coexistence of two conformational species in solutions. The slow dissociation rate corresponds to oligonucleotides in the dimeric duplex form, whereas the fast rate occurs with those in the hairpin conformation. The increased relative contribution of the faster component at higher temperatures is consistent with the more favorable thermal stability of the hairpin form. Studies with d(ATGCAT-TTT-ATGCAT) and d(ATGCAT-AAA-ATGCAT), which exist predominantly in the hairpin conformation, indicate that 7-AM-ACTD dissociates from these oligomers single-exponentially with rate constants comparable to or less than those obtained for the dimeric duplex of d(ATGCATATGCAT). Equilibrium binding titrations suggest that ACTD binds to hairpins as strongly as to the related dimeric duplexes, suggesting that the stacking geometry of the G·C base pairs at the dG-dC intercalating site of the hairpin stem is not greatly different from that of the dimeric duplex. The considerable variation in the dissociation rates of 7-AM-ACTD from hairpins, however, reflects the varying degrees of DNA minor-groove distortion of the stem duplex resulting from the hairpin loop formation and consequent interactions with the pentapeptide rings of ACTD. The plausibility of our interpretation is further supported by results from electrophoretic measurements, thermal melting profiles, and additional studies with hairpins containing a CGCG or GCGC stem.

Actinomycin D (ACTD) is an antitumor antibiotic that contains a 2-aminophenoxazin-3-one chromophore and two cyclic pentapeptide lactones. This drug binds strongly to and dissociates slowly from native duplex DNA with multiexponential decay (Mueller & Crothers, 1968). Its intercalative mode of DNA binding and its preference for the dG-dC sequence have been firmly established (Sobell & Jain, 1972; Patel, 1974; Krugh et al., 1977; Brown et al., 1984; Wilson et al., 1986; Chen, 1988a; Kamitori & Takusagawa, 1992). Recent studies (Lane et al., 1983; Scamrov & Beabealashvilli, 1983; Aivasashville & Beabealashvilli, 1983; Fox & Waring, 1984; Duffy & Lindell, 1985; Phillips & Crothers, 1986; Chen, 1988b; Rill et al., 1989; Goodisman et al., 1992) aimed at elucidating the base sequence specificity of ACTD binding beyond this dinucleotide sequence have established that the adjacent bases (sequences) can profoundly affect the binding and kinetic properties of ACTD at this site. Studies with oligonucleotides each containing single self-complementary (Chen, 1988b) or non-self-complementary (Chen, 1992) -XGCY- binding site revealed that ACTD dissociates from these oligomers single-exponentially with rates that are strongly dependent on the nature of the X and Y bases. This evidence supports and extends the site-heterogeneity model (Krugh et al., 1980) for rationalizing the multiexponential nature of drug dissociation from native DNA. At the tetranucleotide sequence level, -TGCA- has been shown to be both a strong binding and a slow dissociation site. To gain further insights into the nature of its DNA binding, studies have now been extended to include oligomers containing more than one -TGCA- site. Taking advantage of the fact that the addition of an amino group at the 7-position of ACTD greatly enhances its luminescence characteristics without significantly altering its intercalative binding affinity to DNA, SDS-induced dissociation kinetic measurements of 7-amino-ACTD from oligonucleotides containing two identical binding sites were investigated. The results are reported herein.

MATERIALS AND METHODS

Oligonucleotides were synthesized with a Biosearch 8600 DNA synthesizer with use of β-cyanoethyl phosphoramidite chemistry. The crude oligomer was purified by strong anion-exchange (SAX) HPLC followed by reverse-phase HPLC as detailed earlier (Chen, 1988a). The purified and lyophilized oligomers were dissolved in 10 mM Tris buffer of pH 8.6 containing 0.1 M NaCl. All experiments were carried out in this buffer unless noted otherwise. Concentrations of these oligomers (per nucleotide) were determined by measuring the absorbance at 260 nm after melting, with use of extinction coefficients obtained via nearest-neighbor approximation using mono- and dinucleotide values tabulated in Fasman (1975). The extinction coefficients used for drug concentration determination are 24500 M^{-1} cm^{-1} at 440 nm for ACTD and 23600 M^{-1} cm^{-1} at 528 nm for 7-amino-ACTD.

Absorption spectra were measured with a Cary 210 spectrophotometric system. Spectral titrations were carried out at 18.5 °C, starting with an ACTD solution and progressive additions of the oligomer stock. Absorbance changes at 427 and 480 nm were used to obtained Scatchard plots. Fluorescence measurements were made with an SLM 48000S system. Scatchard plots via fluorescence titrations of 7-amino-ACTD (7-AM-ACTD) were made by integrating emission spectral intensities from 580 to 780 nm while exciting the sample at 560 nm. Fluorescence kinetic measurements of 1% sodium dodecyl sulfate- (SDS-) induced dissociation were

† Supported by Grant CA-42682 and by a subproject of Minority Biomedical Research Support (MBRS) Grant S06GM0892.

‡ MBRS undergraduate student participants.

0006-2960/93/0432-5554$04.00/0

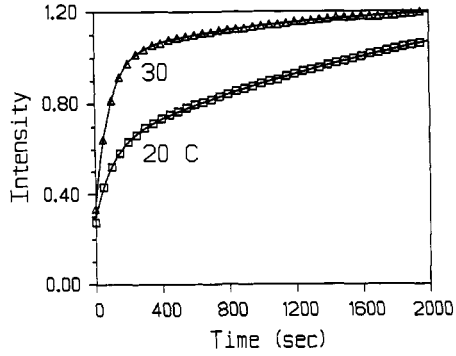

FIGURE 1: Time-dependent fluorescence intensity changes for the 1% SDS-induced dissociation of 7-AM-ACTD (4 μM) from d(ATGCATATGCAT) (50 μM/nucleotide) at 20 and 30 °C. Emission intensities were monitored at 600 nm with the excitation wavelength being placed at 560 nm. Connected curves are those of nonlinear least-squares fits with double exponentials, and the extracted rate parameters are shown in Table I.

carried out by monitoring emission intensity changes at 600 nm using a stirrer accessory.

Thermal denaturation experiments of each oligomer and its drug–DNA mixture were carried out with 1-cm semimicro cells by monitoring absorbances at 260 nm and collecting data at 15-s intervals with an Apple II microcomputer. A heating rate of 0.5 °C/min was maintained by a Neslab RTE-8 refrigerated circulating bath and an EPT-4RC temperature programmer. Numerical differentiations were performed to obtain differential melting profiles from which melting temperatures were deduced. Kinetic rate parameters were obtained using a nonlinear least-squares fit program of Micromath (Salt Lake City, UT).

Electrophoretic measurements were made on a Pharmacia Phast System using 20% polyacrylamide gels at 200 V with appropriate pre- and postloading run times at different temperatures. PhastGel native buffer strips containing 0.25 M Tris at pH 8.8 were used and the gels were developed by silver staining.

RESULTS

d(ATGCATATGCAT) Exhibits Double-Exponential ACTD Dissociation Kinetics and a Biphasic Melting Profile. SDS-induced 7-AM-ACTD dissociation from DNA can be conveniently monitored by the fluorescence intensity increase at 600 nm. Time-dependent fluorescence intensity changes for the dissociation of 7-AM-ACTD from d(ATGCATATGCAT) at two different temperatures (20 and 30 °C) are shown in Figure 1. Despite the fact that this dodecamer is self-complementary and contains two identical dG-dC binding sites, the kinetic data cannot be adequately described by a single-exponential decay. This can be seen more clearly with a semilogarithmic plot of fluorescence intensity change vs time, as shown in Figure 2. A composite of two straight lines is quite apparent for both temperatures, with the contribution from the faster component becoming much more prominent at the higher temperature. Results from nonlinear least-squares fits indicate that the sum of square deviation improves by more than an order of magnitude when two rate constants instead of a single-exponential are used to fit the kinetic data. However, no significant improvement is seen with the addition of a third rate constant. The excellent nonlinear least-squares fits with two rate constants (connected curves) are clearly evident in Figure 1. The extracted rate parameters suggest that the contribution from the faster component amounts to about 28% at 20 °C, which increases to nearly 65% at 30 °C.

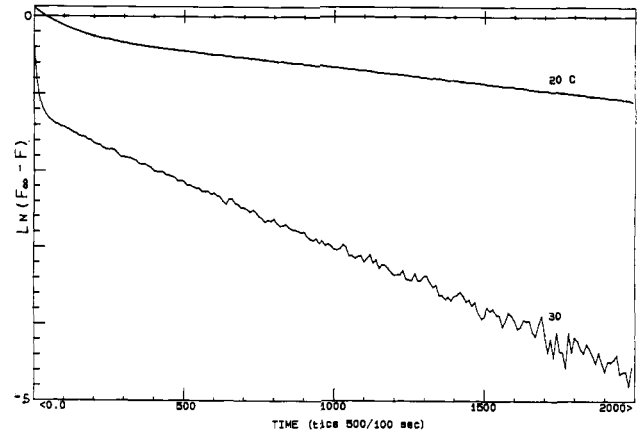

FIGURE 2: Semilogarithmic plots of the time-dependent fluorescence intensity changes at 600 nm, $F_\infty - F$, for the SDS-induced dissociation of 7-AM-ACTD from d(ATGCATATGCAT) at 20 and 30 °C.

Table I: Comparison of SDS-Induced 7-AM-ACTD Dissociation Rate Constants and Their Relative Contributions As Extracted from Nonlinear Least-Squares Fits

oligomer	t (°C)	k_1 (s^{-1})	%	k_2 (s^{-1})	%
d(ATGCATATGCAT)	20	9.2×10^{-3}	28	3.5×10^{-4}	72
	30	9.3×10^{-2}	65	4.9×10^{-3}	35
d(ATGCAT-T-ATGCAT)	20	3.9×10^{-3}	68	1.6×10^{-3}	32
	30	4.3×10^{-2}	~100		
d(ATGCAT-A-ATGCAT)	20	8.5×10^{-3}	79	5.5×10^{-4}	21
	30	8.3×10^{-2}	~100		

The rate constants and their relative contributions are summarized in Table I.

The coexistence of two rate processes when linked with the earlier observation of a single-exponential decay of ACTD from a duplex with a single site (Chen, 1988b, 1992) suggests the possibility of another conformational species in addition to the dimeric duplex. The self-complementary nature of this dodecameric sequence makes the hairpin conformation the most logical candidate. Further, since the relative contribution of the faster component was observed to increase at a higher temperature, it appears that the faster process corresponds to drug molecules dissociating from the hairpin species. Consequently, the slower one must correspond to dissociation from the dimeric duplex. This is the logical conclusion since the hairpin form is thermally more stable than the corresponding dimeric duplex.

Further support for the simultaneous presence of two conformational species in solutions comes from the observed biphasic melting profile of d(ATGCATATGCAT), with melting temperatures near 25 and 50 °C, respectively (Figure 3). The cooling curve (not shown) exhibits no hysteresis for the higher temperature transition but shows considerable lag at the lower temperature transition. The complete reversibility of the higher temperature transition is in accord with the rapid intramolecular process of hairpin formation, whereas the slow renaturation at the lower temperature transition is consistent with the intermolecular event of dimeric duplex formation. The biphasic nature of the melting profile is retained in the presence of ACTD with melting temperature increases of roughly 20 °C for both transitions, suggesting that the drug binding stabilizes both hairpin and dimeric duplexes to about the same extent.

Kinetic Behavior of Oligomers with an Added Central Base. To further support our thesis, SDS-induced 7-AM-ACTD dissociation from 13-mers d(ATGCAT-T-ATGCAT) and d(ATGCAT-A-ATGCAT) was also investigated at two different temperatures. It was reasoned that the presence of

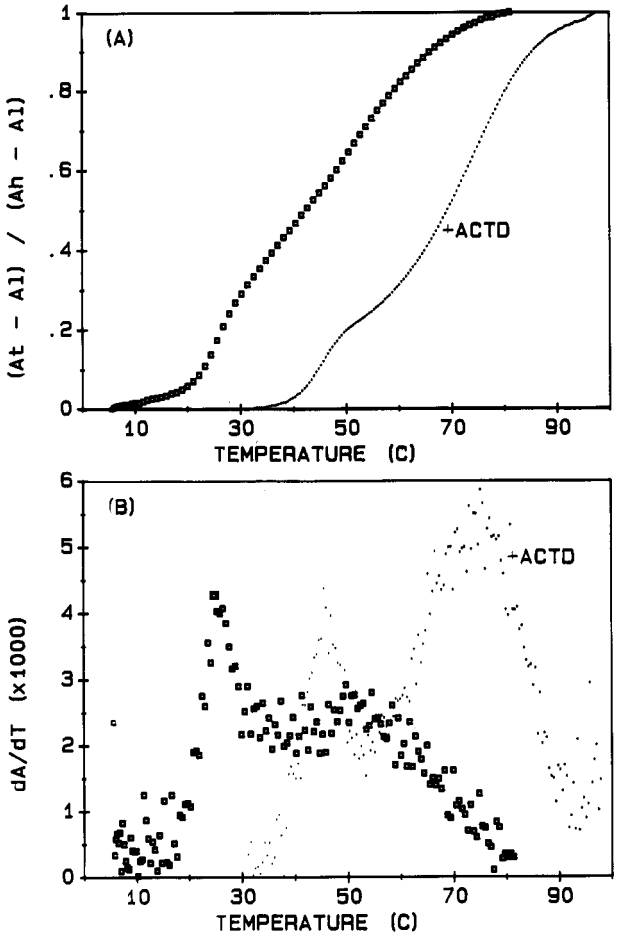

FIGURE 3: Thermal denaturation (A) and differential melting (B) profiles of d(ATGCATATGCAT) in the absence (squares) and in the presence (dotted curve) of ACTD. Absorbance monitored at 260 nm in 10 mM Tris buffer and pH 8.6 containing 0.1 M NaCl. A_h, A_l, and A_t are absorbances at high and low temperatures and at t, respectively.

an extra base at the center would result in a base-pair mismatch. Thus, the dimeric duplex would become less stable and thereby facilitate the hairpin formation. Indeed, the dissociation kinetics most certainly are not single exponentials at 20 °C. Further, the contributions from the faster component increase to more than 68% for the two 13-mers, as compared to 28% from the self-complementary d(ATGCATATGCAT). Additionally, the rate processes of the two 13-mers become single exponentials at 30 °C, which is to be expected as the ACTD–hairpin complexes predominate at this temperature. Rate parameters extracted from the least-squares fits are included in Table I for comparison. The table shows a slightly slower rate for the fast component of the two 13-mers as compared to that of d(ATGCATATGCAT). This is probably attributable to more facile hairpin formation by the 13-mers. Further, a comparison of the rates for the slow component of the 13-mers with that of d(ATGCATATGCAT) reveals a significant increase in the rate for the oligomers with the central base-pair mismatch. This is probably due to the reduced stability of the dimeric duplex resulting from the mismatch.

ACTD Dissociates Single-Exponentially from Oligomers Containing Three Centrally Added Bases. To gain additional support for our interpretation, oligomers which exist exclusively in the hairpin form were synthesized. The dissociation kinetics of 7-AM-ACTD from d(ATGCAT-TTT-ATGCAT) and d(ATGCAT-AAA-ATGCAT) were investigated at three different temperatures and were found to be strictly single

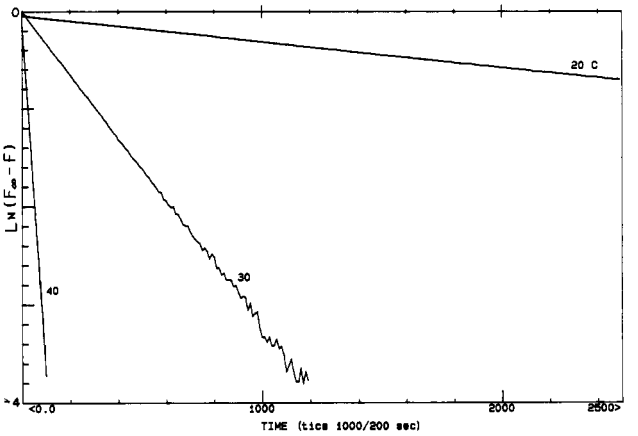

FIGURE 4: Semilogarithmic plots for the 1% SDS-induced dissociation kinetic data of 7-AM-ACTD in d(ATGCAT-TTT-ATGCAT) solutions at three different temperatures.

Table II: Comparison of Temperature-Dependent 7-AM-ACTD Dissociation Rate Constants for Two 15-mers Which Form Exclusively Hairpins

oligomer	t (°C)	k (s^{-1})
d(ATGCAT-TTT-ATGCAT)	20	2.8×10^{-4}
	30	3.2×10^{-3}
	40	3.5×10^{-2}
d(ATGCAT-AAA-ATGCAT)	20	3.4×10^{-4}
	30	5.4×10^{-3}
	40	7.8×10^{-2}

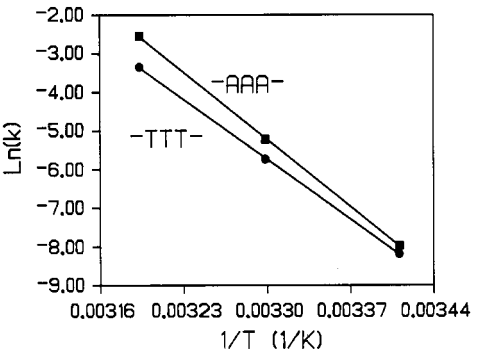

FIGURE 5: Arrhenius plots of SDS-induced dissociation of 7-AM-ACTD from d(ATGCAT-TTT-ATGCAT) and d(ATGCAT-AAA-ATGCAT).

exponentials, as evident from the straight lines exhibited by the semilogarithmic plots in Figure 4. The corresponding rate constants extracted from linear least-squares fits are summarized in Table II. An outstanding fact is that the dissociation rates at 20 °C for these two 15-mers are considerably slower than the fast components but are comparable to (or even slower than) the slower components of the three previously studied oligomers. Arrhenius plots with these temperature-dependent rate constants are shown in Figure 5. It is apparent that excellent linear fits are obtained from the data points which yield activation energies of 44.1 and 49.5 kcal/mol for the -TTT- and -AAA- oligomers, respectively.

The possible presence of the dimeric species for these oligomers was investigated by kinetic measurements in solutions containing an order of magnitude higher DNA concentration to facilitate the intermolecular events. SDS-induced drug dissociation kinetics in these solutions, however, can all be adequately described by single-exponential decays, suggesting negligible, if any, contributions from the dimeric form. This conclusion is also supported by the absence of the dimeric bands in electrophoretic experiments (see later) where

Table III: Comparison of Equilibrium Binding Constants and Binding Densities for ACTD at 18.5 °C As Extracted from Absorption Spectral Titrations

oligomer	K (M^{-1})	n (per strand)
d(ATGCATATGCAT)	1.6×10^7	1.2
d(ATGCAT-T-ATGCAT)	3.9×10^7	1.2
d(ATGCAT-A-ATGCAT)	2.3×10^7	1.2
d(ATGCAT-TTT-ATGCAT)	3.3×10^7	1.1
d(ATGCAT-AAA-ATGCAT)	1.4×10^7	1.3

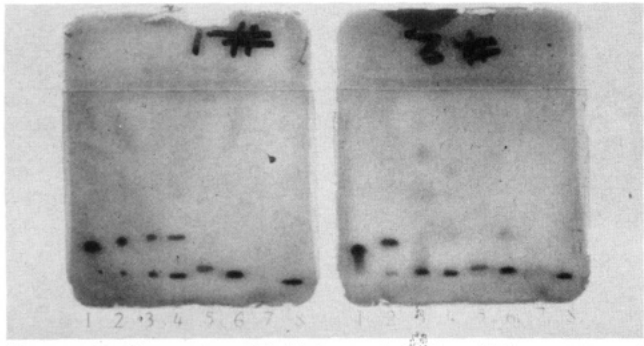

FIGURE 6: Comparison of gel-electrophoretic mobility patterns of selected oligomers at 4 °C (panel A) and 14 °C (panel B). Lanes 1, d(ATACGCGTAT); lanes 2, d(ATGCATATGCAT); lanes 3, d(ATGCAT-T-ATGCAT); lanes 4, d(ATGCAT-A-ATGCAT); lanes 5, d(ATGCAT-TTT-ATGCAT); lanes 6, d(ATGCAT-AAA-ATGCAT); lanes 7, d(CGCG-TT-CGCG); lanes 8, d(GCGC-TT-GCGC). Oligomer concentrations (per nucleotide) range from 0.5 to 1.5 mM. Experiments were run on 20% polyacrylamide PhastGels at 200 V and run times of 115 V·h at 4 °C, 70 V·h at 14 °C, and 55 V·h at 24 °C, respectively. PhastGel native buffer strips containing 0.25 M Tris at pH 8.8 were used, and the gels were prerun for appropriate lengths of time prior to sample loading. The gels were developed with silver staining.

the oligomer concentrations are considerably higher than those of the optical experiments.

It should also be noted that some kinetic measurements were also made in a Tris buffer of pH 7.8 containing 0.1 M NaCl. There were no appreciable differences in results when using this buffer in lieu of the pH 8.6 buffer.

Equilibrium Binding Titrations Suggest Strong ACTD Binding for All the Oligomers Studied. To see if the hairpins bind to the drug as strongly as the dimeric duplexes, spectral titrations with ACTD were also carried out at 18.5 °C for these oligomers. The results are summarized in Table III. The results reveal equilibrium binding constants of the order of 10^7 M^{-1} and binding densities of roughly one drug molecule per strand (or two per dimeric duplex) for all the oligomers studied. Interestingly, the ACTD binding affinities of exclusively hairpin oligomers are not greatly different from those of the dimeric duplexes. This conclusion is also supported by the absence of unusual curvatures arising from allosteric transitions and differential binding affinities of the two different conformations in the Scatchard plots (not shown) of d(ATGCATATGCAT) and the two 13-mers.

Electrophoretic Evidence of Hairpin Formation. To gain more direct evidence for the existence of hairpin conformations and their drug complexes, electrophoretic measurements were made for the oligomers both in the absence and in the presence of ACTD. Electrophoretic mobilities of selective oligomers at two different temperatures are compared in Figure 6. Two electrophoretic bands are apparent at 4 °C (panel A) for d(ATGCATATGCAT) (lane 2). One band moves significantly faster but is of lower intensity than that of another component which moves slightly slower than the band corresponding to a decameric duplex (lane 1). Thus, the slower

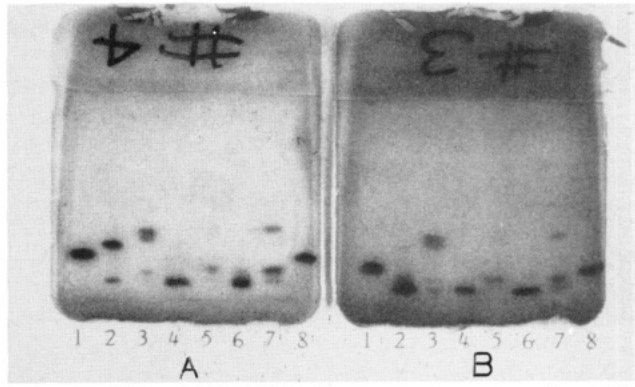

FIGURE 7: Effects of ACTD binding on the electrophoretic mobility patterns at 14 °C (panel A) and 24 °C (panel B). Lanes 1, d(ATAGGCCTAT); lanes 2, d(ATGCATATGCAT); lanes 3, d(ATGCATATGCAT) in the presence of 82 μM ACTD; lanes 4, d(ATGCAT-T-ATGCAT); lanes 5, d(ATGCAT-T-ATGCAT) + 82 μM ACTD; lane 6, d(ATGCAT-A-ATGCAT); lanes 7, d(ATGCAT-A-ATGCAT) + 82 μM ACTD; lanes 8, d(ATACCGGTAT). Oligomer concentration ranges from 0.7 to 1.5 mM.

component is designated to be that of dimeric duplex, whereas the faster component is attributed to that of the hairpin species. Similar electrophoretic mobility patterns are also observed for d(ATGCAT-T-ATGCAT) (lane 3) and d(ATGCAT-A-ATGCAT) (lane 4), except the two bands are of roughly equal intensities. The predominance of the hairpin form in both d(ATGCAT-TTT-ATGCAT) (lane 5) and d(ATGCAT-AAA-ATGCAT) (lane 6), even at this low temperature, is evidenced by the appearance of single bands only, which manifest nearly equal mobility to those of the fast components of the 12- and 13-mers. Although d(ATGCATATGCAT) still exhibits two bands with higher intensity for the slower band at 14 °C (panel B), the slower components for both 13-mers nearly disappear with a concomitant appearance of trailing tails at the faster moving bands. This suggests that the dimeric duplexes of the 13-mers have mostly melted. The d(ATGCATATGCAT), on the other hand, exhibits fading of the slower band and the appearance of a trailing tail at the faster band only at 24 °C (not shown). These results are consistent with those expected for solutions of these oligomers: the coexistence of dimeric duplex and hairpin species at 4 °C for the 12- and 13-mers and the exclusive presence of hairpin species for the 15-mers.

The effect of ACTD binding on the gel mobility patterns at 14 and 24 °C are shown in Figure 7. Both dimeric duplex and hairpin bands have clearly been retarded (compare lanes 2, 4, and 6 with 3, 5, and 7, respectively), indicating ACTD binding to both species. It is interesting to note the presence of two retarded bands for the slower component of d(ATGCATATGCAT) (lane 3). The first band corresponds to the dimeric duplex with one drug molecule bound to it, while the second one shows retardation by two drug molecules. Also of interest is the prominent presence of the drug–DNA bands (see lane 7, in particular) at these temperatures, despite the fact that corresponding DNA bands for the two 13-mers are absent (lanes 4 and 6). These results are consistent with the observed 20 °C increase in the melting temperatures of both dimeric and hairpin species. Hence, the significant presence of the dimeric duplex–drug complex is possible at these temperatures. Additionally, the rates of ACTD dissociation from the dimeric duplex are considerably slower than from the hairpins in these oligomers. The more prominent presence of the slow dimeric duplex–ACTD band of d(ATGCAT-A-ATGCAT), in contrast to that of d(ATGCAT-T-ATGCAT), appears to be consistent with the slower dissociation rate of

Table IV: Comparison of SDS-Induced 7-AM-ACTD Dissociation Rates and Their Relative Contributions for Hairpins Containing a CGCG or GCGC Stem

oligomer	k_1 (s^{-1})	%	k_2 (s^{-1})	%
d(CGCG-TT-CGCG)	1.2×10^{-1}	26	4.5×10^{-2}	74
d(CGCG-TTT-CGCG)	4.6×10^{-2}	18	1.8×10^{-2}	82
d(GCGC-TT-GCGC)	4.2×10^{-1}	5	7.7×10^{-2}	95
d(GCGC-TTT-GCGC)	9.5×10^{-2}	76	9.1×10^{-3}	24
d(GCG-TTT-CGC)	2.4×10^{-1}	100		

the slow component of the -A- than that of the -T- oligomer (see Table I).

Studies of Hairpins with CGCG and GCGC Stems. To gain further insights, studies with hairpins of the form d(CGCG-T_n-CGCG) and d(GCGC-T_n-GCGC), where n = 2 and 3, were also made. Although the dissociation kinetic results at 20 °C can be approximated fairly well by single-exponential decays, better results are obtained with double-exponential fits. The extracted rate constants along with their relative contributions are shown in Table IV. However, due to the rapidity of these kinetics, one should not rely too much upon such a decomposition in the absence of stopped-flow experiments and only the relative rates among the oligomers should be compared. It is to be noted that the electrophoretic evidence (see lanes 7 and 8 of Figure 6) indicates that even at 4 °C the two -TT- oligomers already exist predominantly in the hairpin form. Thus, if multiexponential rate processes were to be observed by rapid mixing techniques, they could have arisen from two binding sites at the GCGC stem or from one binding site and a possible end stacking for the CGCG stem. However, the general trend of the rate decrease as one goes from -TT- to -TTT- is consistent with the more facile loop formation. A rate increase of more than a factor of 5 from d(CGCG-TTT-CGCG) to d(GCG-TTT-CGC) has also been observed.

DISCUSSION

The presence of two ACTD dissociation rate processes and their relative contributions in d(ATGCATATGCAT), d(ATGCAT-T-ATGCAT), and d(ATGCAT-A-ATGCAT) at 20 °C can be attributed to the coexistence of both the dimeric duplex and hairpin species. The faster rate process corresponds to the drug dissociating from the hairpin stem, and its enhanced contribution at higher temperatures is consistent with the more favorable thermal stability of this form compared to the corresponding dimeric species. The strong ACTD binding and its slow single-exponential dissociation from d(ATGCAT-TTT-ATGCAT) and d(ATGCAT-AAA-ATGCAT), which are predominantly in the hairpin form, indicate that ACTD binds strongly to hairpins and its rate of dissociation can be comparable to those of dimeric duplexes. The fact that the hairpin duplex stem binds ACTD as strongly as dimeric duplex suggests that the stacking geometry of the G·C base pairs at the dG-dC intercalating site of the hairpin does not differ greatly from that of the dimeric duplex. The considerable variation in the dissociation rates of the hairpins, however, indicates that some of the minor-groove environments of the hairpin duplexes may have been significantly distorted by the loop formation. Indeed, comparison of the rate constants reveals that 7-AM-ACTD dissociation from the hairpin of d(ATGCATATGCAT) is somewhat faster than those of d(ATGCAT-T-ATGCAT) and d(ATGCAT-A-ATGCAT), which in turn are at least an order of magnitude faster than those of d(ATGCAT-TTT-ATGCAT) and d(ATGCAT-AAA-ATGCAT). The slowness of the drug dissociating from the latter two oligomers suggests that hairpins can easily be formed with a three-base loop and the minor groove of the duplex stems is not greatly distorted near the dG-dC binding region so that the cyclic pentapeptide rings can be fit snugly. On the other hand, the formation of hairpins with three-base loops by the two 13-mers somewhat distorts the minor-groove environment near the binding site. Additionally, the hairpin formation for d(ATGCATATGCAT) most likely involves a two-base -TA- or four-base -ATAT- loop, which considerably distorts the stem duplex near the loop so that secure anchorage becomes difficult for one of the pentapeptide rings. The enhanced 7-AM-ACTD dissociation rates from d(CGCG-TT-CGCG) and d(GCGC-TT-GCGC), as compared to those from the corresponding d(CGCG-TTT-CGCG) and d(GCGC-TTT-GCGC), are consistent with such an interpretation. The 5-fold increase in the dissociation rate for d(GCG-TTT-CGC) as compared to d(CGCG-TTT-CGCG) can be attributed to the inability of the drug to anchor the pentapeptide ring at the nonlooping end.

Finally, our dissociation kinetic results appear to suggest that a hairpin with a single binding site and a dimeric duplex with two identical sites both exhibit single-exponential decays. Such a simple correlation, however, can be somewhat misleading. Since the phenoxazone chromophore is not symmetric, ACTD can intercalate into the binding site via two distinct orientations differing by a 180° rotation. In view of the fact that a hairpin does not possess C_2 symmetry, the two complexes formed will not be equivalent. Furthermore, there can be three possible ways of arranging ACTD at the two dG-dC binding sites in a duplex such as d(ATGCATATGCAT)$_2$. Two of these arrangements possess C_2 symmetry, while the third one is unsymmetrical (Jones et al., 1988). Therefore, the observation of a single-exponential decay of an exclusively hairpin oligomer with a unique binding site or a duplex with two identical binding sites may possibly be due to either the predominance of one of the complexes and/or the near identical pentapeptide interactions with the minor groove in these complexes. The NMR evidence of more than one complexes in some oligomers (Jones et al., 1988) coupled with our observed considerable variation in the rates of ACTD dissociation with the nature of hairpin loop formation appear to argue in favor of the latter possibility. This underscores the critical role played by the pentapeptide ring–minor-groove interactions in the kinetic processes.

ACKNOWLEDGMENT

We thank D. Dunson for her careful reading of the manuscript.

REFERENCES

Aivasashvilli, V. A., & Beabealashvilli, R. S. (1983) *FEBS Lett. 160*, 124–128.

Brown, S. C., Mullis, K., Levenson,C., & Shafer, R. H. (1984) *Biochemistry 23*, 403–408.

Chen, F.-M. (1988a) *Biochemistry 27*, 1843–1848.

Chen, F.-M. (1988b) *Biochemistry 27*, 6393–6397.

Chen, F.-M. (1992) *Biochemistry 31*, 6223–6228.

Duffy, J. J., & Lindell, T. J. (1985) *Biochem. Pharmacol. 34*, 1854–1856.

Fasman, G. D., Ed. (1975) *CRC Handbook of Biochemistry and Molecular Biology*, 3rd ed., Vol. I, p 589, Chemical Rubber Publishing Co., Cleveland, OH.

Fox, K. R., & Waring, M. J. (1984) *Nucleic Acids Res. 12*, 9271–9285.

Goodisman, J., Rehfuss, R., Ward, B., & Dabrowiak, J. C. (1992) *Biochemistry 31*, 1046–1058.

Jones, R. L., Scott, E. V., Zon, G., Marzilli, L. G., & Wilson, W. D. (1988) *Biochemistry 27*, 6021–6026.
Kamitori, S., & Takusagawa, F. (1992) *J. Mol. Biol. 225*, 445–456.
Krugh, T. R., Mooberry, E. S., & Chiao, Y.-C. C. (1977) *Biochemistry 16*, 740–755.
Krugh, T. R., Hook, J. W., Balakrishnan, M. S., & Chen. F.-M. (1980) in *Nucleic Acids Geometry and Dynamics* (Sarma, R. H., Ed.) pp 351–366, Pergamon, New York.
Lane, M. J., Dabrowiak, J. C., & Vouurrnakis, J. N. (1983) *Proc. Natl. Acad. Sci. U.S.A. 80*, 3260–3264.
Muller, W., & Crothers, D. M. (1968) *J. Mol. Biol. 35*, 251–290.
Patel, D. J. (1974) *Biochemistry 13*, 2396–2402.
Phillips, D. R., & Crothers, D. M. (1986) *Biochemistry 25*, 7355–7362.
Rill, R. L., Marsch, G. A., & Graves, D. E. (1989) *J. Biomol. Struct. Dyn. 7*, 591–605.
Scamrov, A. V., & Beabealashvilli, R. Sh. (1983) *FEBS Lett. 164*, 97–101.
Sobell, H. M., & Jain, S. C. (1972) *J. Mol. Biol. 68*, 21–34.
Wilson, W. D., & Jones, R. L., Zon, G., Scott, E. V., Banville, D. L., & Marzille, L. G. (1986) *J. Am. Chem. Soc. 108*, 7113–7119.